



Cite this: DOI: 10.1039/d5gc02625c

Recycling of anhydride-cured epoxy resin-based carbon fiber-reinforced composites via a β -phenethyl alcohol/TBD catalytic system

Renlong Min,[†] Chenyu Zhang, ^{*,†} Haijuan Kong, Shuo Liu and Ziyao Peng

Carbon fiber-reinforced polymers (CFRPs) are widely applied due to their outstanding mechanical properties. However, the intrinsic difficulty in recycling their thermoset resin matrix has led to serious environmental pollution and resource waste, becoming a major bottleneck hindering the sustainable development of CFRPs. In this study, a green and efficient chemical recycling strategy was developed by constructing a synergistic catalytic system composed of β -phenylethanol and 1,5,7-triazabicyclo[4.4.0]dec-5-ene (TBD), enabling the rapid degradation of anhydride-cured epoxy-based CFRPs under mild conditions (190 °C, atmospheric pressure). By optimizing the mass ratio of the catalyst to the composite material [TBD : CFRP (wt : wt) = 1 : 3.27], nearly complete resin degradation (>99%) was achieved within 2 hours. The reclaimed carbon fibers retained up to 93.2% of their original single-fiber tensile strength. X-ray photoelectron spectroscopy (XPS) and X-ray diffraction (XRD) analyses confirmed that no significant deterioration occurred in the surface chemical functionalities or the degree of graphitization of the reclaimed fibers compared to the pristine ones. This work offers a simple, efficient, and environmentally friendly solution for the closed-loop recycling of thermoset-based CFRPs.

Received 26th May 2025,
 Accepted 28th July 2025
 DOI: 10.1039/d5gc02625c
rsc.li/greenchem

Green foundation

1. Our work provides a novel and efficient chemical recycling approach for anhydride-cured epoxy resin-based carbon fiber-reinforced polymers (CFRPs), which are notoriously difficult to recycle due to their cross-linked thermoset matrix. By employing a synergistic catalytic system of β -phenylethanol and TBD under mild conditions (190 °C, atmospheric pressure), we achieved rapid degradation of the resin without damaging the carbon fibers. This contributes to the green chemistry field by promoting resource circularity, reducing hazardous waste, and replacing energy-intensive pyrolysis or harsh chemical treatments with a safer, more environmentally friendly alternative.
2. Quantitatively, our method achieves >99% degradation efficiency of the epoxy matrix within 2 hours. The reclaimed carbon fibers retain up to 93.2% of their original tensile strength, with negligible surface oxidation or structural damage, as confirmed by XPS and XRD analyses. Qualitatively, the process uses non-toxic, readily available solvents and catalysts, operates at atmospheric pressure, and avoids secondary pollution. This represents a significant advancement in the chemical recyclability of high-performance thermoset composites.
3. Future work could focus on developing fully bio-based or recyclable alternatives to β -phenylethanol and TBD to further reduce environmental impact. Additionally, improving solvent recovery and reusability, scaling the process for industrial application, and integrating the recovered fibers into closed-loop manufacturing systems will elevate the sustainability and commercial viability of the method. Life cycle assessment (LCA) could also provide a comprehensive evaluation of the environmental benefits compared to conventional disposal methods.

Introduction

CFRPs are composed of a high-performance carbon fiber reinforcement (carbon content >90%) embedded in an epoxy resin matrix.¹ Owing to their high strength, high stiffness, and lightweight characteristics, CFRPs have been widely employed in aerospace, automotive, and wind energy applications.² Global statistics

indicate that the amount of CFRP waste surged from 27.2 kilotons in 2017 to 45 kilotons in 2022, and projections suggest that the cumulative volume will reach 983 kilotons by 2050.^{3,4} Approximately 40% of the total CFRP waste is attributed to manufacturing scrap.⁵ The cured thermosetting epoxy resin forms a highly cross-linked three-dimensional network, which significantly hinders the direct recycling of CFRPs. As a result, current recycling approaches primarily rely on incineration or landfilling, leading to the waste of carbon fibers that still possess excellent mechanical properties and causing severe environmental pollution.³

To address the pressing issues of resource scarcity and environmental pollution, the development of efficient re-

School of Materials Science and Engineering, Shanghai University of Engineering Science, Songjiang District, Shanghai 201620, People's Republic of China.
 E-mail: zhangcy@sues.edu.cn; Tel: +13122673217

[†]These authors contributed equally to this work.

cycling technologies for CFRPs is urgently needed. Currently, the primary recycling approaches include mechanical, thermal, and chemical methods.⁶ Mechanical recycling is suitable only for uncontaminated materials. The low-density fibers obtained through crushing and separation processes often suffer from degraded mechanical properties and are typically reused only as fillers or reinforcement agents in other composite matrices.^{7,8} Thermal recycling is currently the most widely implemented method at the industrial scale, primarily involving pyrolysis (350–700 °C) and fluidized bed processes.⁹ Pyrolysis allows for the recovery of relatively clean carbon fibers; however, it often results in fiber shortening and a tensile strength retention of only 70–75%.^{10,11} The fluidized bed process utilizes a heated silica sand bed and high-temperature air to fluidize the composite and thermally decompose the resin matrix.¹² Hot air fluidization enables rapid heating of the composite material and promotes oxidative decomposition of the epoxy resin, effectively liberating carbon fibers in a fluffy state from the resin matrix.¹³ Compared to pyrolysis, fluidized bed processing causes more severe damage to carbon fibers. In addition, thermal recycling methods face several critical limitations, including incomplete fiber recovery, high operational costs, substantial energy consumption, and the emission of hazardous gases such as CO, NO_x, SO₂, and SO₃, which pose significant risks to environmental and human health.^{13,14}

Solvent-based recycling degrades the resin matrix *via* alcoholysis, hydrolysis, or functional group substitution reactions under controlled temperature (typically below 400 °C) and pressure, offering notable advantages such as low energy consumption and excellent retention of fiber integrity.¹⁵ However, conventional solvent-based methods still face significant limitations. The high consumption of solvents not only increases economic costs but also poses risks of secondary environmental pollution. In addition, these methods typically exhibit low degradation efficiency, often requiring 12–24 hours to achieve over 90% resin removal.¹⁶ Furthermore, under high-temperature conditions (>250 °C), severe oxidation occurs on the surface of carbon fibers, leading to a tensile strength loss of 15–30%, which greatly restricts the industrial applicability of solvent-based recycling strategies.^{17,18}

To overcome the limitations of conventional recycling methods, the introduction of the TBD catalytic system represents a significant advancement.¹⁹ As a bifunctional organo-catalyst, TBD enables over 95% resin degradation under mild conditions (180–200 °C) while preserving more than 90% of the original fiber tensile strength. This is achieved through a synergistic mechanism involving Brønsted base-activated hydroxyl groups and nucleophilic cleavage of ester bonds. For example, Wu and co-workers reported a TBD/ethylene glycol (EG) system that enabled complete carbon fiber recovery *via* transesterification at 180 °C for 6 h, with a single-filament strength retention of 93.2%.²⁰ Similarly, Bruna *et al.* achieved 89% epoxy resin degradation in aerospace-grade CFRPs at just 95 °C by combining UVB pretreatment with nitric acid catalysis, demonstrating the feasibility of low-temperature catalytic

strategies.²¹ Although elevated temperatures can accelerate resin decomposition—as demonstrated by Chaabani *et al.*, who achieved 98.95% degradation at 280 °C for 30 min and 97.15% at 400 °C for 15 min using subcritical (280–350 °C) and supercritical (400–600 °C) hydrothermal conditions at 25 MPa—higher temperatures also intensify graphitization defects in carbon fibers, leading to a 12% reduction in mechanical performance. This underscores the trade-off between degradation efficiency and fiber integrity.²² In contrast, mechanical recycling and pyrolysis introduce more extensive structural damage. Mechanical treatments increase fiber breakage rates by 20–50% and surface roughness by 150–300% (*R_a*), while pyrolysis decreases graphitization and reduces interfacial bonding strength by 40–60%. These findings further highlight the value of mild catalytic degradation approaches for sustainable and high-performance CFRP recycling.^{23,24}

Inspired by the aforementioned advancements, this study presents a simple yet efficient method for recycling carbon fibers from anhydride-cured epoxy resin (DGEBA/MNA)-based carbon fiber-reinforced polymers (CFRPs). The method utilizes a β -phenethyl alcohol/TBD system to achieve 100% carbon fiber recovery at 190 °C, offering the dual benefits of high-efficiency degradation and low-damage recovery. The recovered fibers exhibit a high similarity in surface microstructure and elemental composition compared to virgin fibers, providing an eco-friendly and economically viable solution for closed-loop CFRP recycling (Fig. 1).

Experimental

Materials

The pultruded carbon spar recovered from a decommissioned wind turbine blade (composed of a carbon fibre panel based on an anhydride-cured epoxy resin), as well as methyl nadic

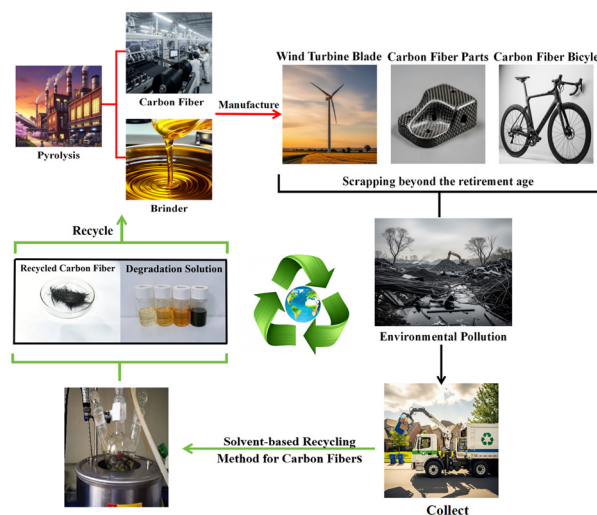


Fig. 1 Production and recycling pathways of carbon fiber reinforced polymer (CFRP) composites.

anhydride (MNA, curing agent), diglycidyl ether of bisphenol A (DGEBA), and copper(II) *N*-methylpyrrolidone-2-carboxylate (CMP) were supplied by Jiangsu Aosheng Composite Materials Technology Co., Ltd. (China). β -Phenethyl alcohol ($C_8H_{10}O$), 1,5,7-triazabicyclo[4.4.0]dec-5-ene (TBD), ethylene glycol ($C_2H_6O_2$), and sodium hydroxide were purchased from Shanghai Aladdin Biochemical Technology Co., Ltd (China) and used as received without further purification (Fig. 2).

Sample preparation

To assess the practical applicability of the recycling method, the self-developed protocol was applied to anhydride-cured carbon fiber composite panels reclaimed from decommissioned wind turbine blades. According to ISO 14127, the carbon fiber mass fraction was determined to be 69%. Prior to recycling, the protective surface coating was mechanically removed, and the panels were precision-cut into standard specimens ($20\text{ mm} \times 10\text{ mm} \times 5\text{ mm}$; average mass: 1.55 g) using a computer numerical control (CNC) milling machine. The specimens were sequentially cleaned by ultrasonic treatment in acetone and ethanol, rinsed with de-ionized water until neutral, and dried at $60\text{ }^\circ\text{C}$ for 24 h. The surface morphology of the prepared samples is shown in Fig. 3. To minimize the environmental influence on material properties, all samples were sealed in polyethylene bags and stored at $25 \pm 2\text{ }^\circ\text{C}$.

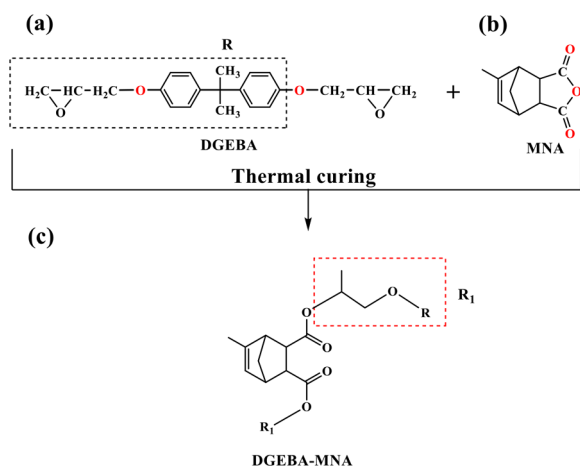


Fig. 2 Schematic illustration of the epoxy resin curing mechanism: (a) molecular structure of diglycidyl ether of bisphenol A (DGEBA), (b) molecular structure of Methyl nadic anhydride (MNA), and (c) proposed molecular structure of the cured DGEBA-MNA network.

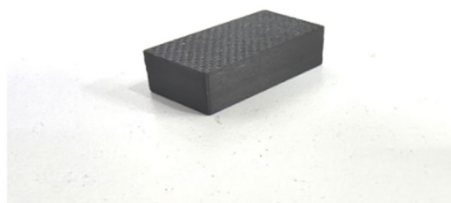


Fig. 3 Morphology of the experimental samples.

Solvent-based recycling process

A schematic illustration of the recycling procedure is provided in Fig. 4. Each experimental run processed a single CFRP specimen. The composite, together with the solvent and catalyst (formulations detailed in Table 1), was loaded into a three-neck round-bottom flask. The reaction vessel was immersed in an oil bath to maintain a constant temperature and was fitted with a reflux condenser and circulating cooling water to prevent solvent loss. The degradation reaction was conducted for 1–2 h. After completion and cooling to ambient temperature, the recovered carbon fibers were separated, thoroughly washed with acetone or ethanol, rinsed three times with de-ionized water, and subsequently dried under vacuum at $80\text{ }^\circ\text{C}$ for 12 h.

The degradation rate (DR) of carbon fibers, along with the results of the control group, was calculated using a predefined equation to provide a preliminary assessment of the solvent's decomposition efficiency and the catalytic performance of the system.

$$DR(\%) = \frac{w_1}{w_2 \times 69\%} \times 100\% \quad (1)$$

where w_1 is the mass of the recovered carbon fibers after decomposition, washing, and drying, and w_2 is the mass of the pristine resin in the composite material.

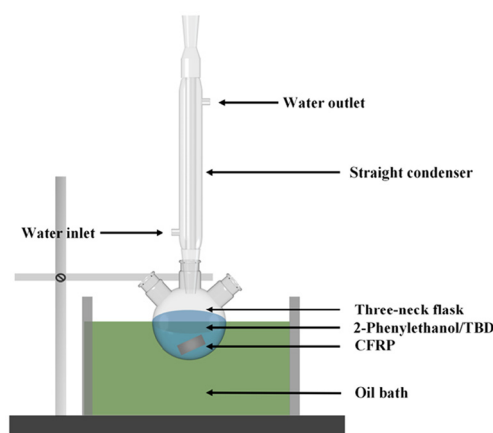


Fig. 4 Schematic diagram of the CFRP recycling process.

Table 1 Recycling conditions and the corresponding results for the β -phenethyl alcohol/TBD system

No.	$C_8H_{10}O$: TBD (wt : wt)	Temperature/ $^\circ\text{C}$	Time/h	DR/%
(A)	20 : 1	150	2	61.65
(B)	30 : 1	150	2	68.56
(C)	50 : 1	150	2	35.45
(D)	20 : 1	180	2	76.39
(E)	30 : 1	180	2	86.77
(F)	50 : 1	180	2	62.44
(G)	20 : 1	190	2	87.18
(H)	30 : 1	190	2	100
(I)	50 : 1	190	2	74.87
(J)	30 : 1	200	2	100

After 48 h of standing, the recycling solution primarily consisted of β -phenethyl alcohol and resin degradation products. To elucidate the degradation mechanism of anhydride-cured epoxy resin in the β -phenethyl alcohol/TBD system, samples of the recycling solution were collected at various stages—before, during, and after the reaction—and the colloidal residues obtained *via* rotary evaporation were also analyzed. The results of these characterization methods are presented and discussed in the following sections.

Characterization

Thermogravimetric analysis (TGA) was conducted using a Mettler Toledo TGA/DSC3+ analyzer (Switzerland) under a nitrogen atmosphere with a heating rate of $10\text{ }^{\circ}\text{C min}^{-1}$ up to $700\text{ }^{\circ}\text{C}$.²⁵ Field-emission scanning electron microscopy (FE-SEM) images were acquired using a Hitachi SU8010 instrument (Japan) to examine the surface morphology of carbon fibers. X-ray photoelectron spectroscopy (XPS) was performed on a Thermo Scientific K-Alpha system (USA) to determine the surface elemental composition and C/O ratio, with the spectra collected in constant analyzer energy mode (pass energy: 30 eV for high-resolution scans).²⁶ Fourier-transform infrared (FTIR) spectroscopy was conducted using a Nicolet iS50 spectrometer (Thermo Fisher Scientific, USA) at a resolution of 4 cm^{-1} over a range of $400\text{--}4000\text{ cm}^{-1}$. Nuclear magnetic resonance (NMR) spectroscopy was carried out using a Bruker Avance III 400 MHz spectrometer (Germany) with DMSO- d_6 as the solvent.

X-ray diffraction (XRD) analysis was performed on a Bruker D8 Advance diffractometer (Germany) equipped with Cu $K\alpha$ radiation ($\lambda = 1.5405\text{ \AA}$) to assess the structural characteristics of the carbon fibers.^{26,27} The key structural parameters of the recycled carbon fibers—including the interlayer spacing, crystallite size, and degree of graphitization—were calculated from the XRD patterns using Bragg's law and the Debye-Scherrer equation.

$$d_{002} = \frac{\lambda}{2 \sin \theta} \quad (2)$$

$$D = \frac{K\lambda}{\beta \cos \theta} \quad (3)$$

where λ represents the wavelength of Cu $K\alpha_1$ radiation (0.15405 nm), θ is the Bragg diffraction angle, and β denotes the full width at half maximum (FWHM) of the (002) diffraction peak. A shape factor (K) of 0.89 was applied in the Debye-Scherrer equation for crystallite size estimation.

Single-fiber tensile tests were performed in accordance with the GB/T 31290-2022 standard using an Instron 5944 microtester (USA) equipped with a 10 N load cell. The gauge length was set to $25 \pm 0.5\text{ mm}$, and the crosshead speed was maintained at 1 mm min^{-1} . The fiber diameters ($7.46 \pm 0.7\text{ }\mu\text{m}$) were determined using scanning electron microscopy (SEM) based on measurements from 100 individual fibers to calculate the cross-sectional area. For each sample, a minimum of 30 specimens were tested. Carbon fibers were elongated to failure, and

the corresponding force-displacement curves were recorded.^{26,28} The tensile strength of each filament was calculated using the following equation:

$$\sigma_b = \frac{4F}{\pi d^2} \quad (4)$$

where d represents the diameter of the fiber, σ_b denotes the tensile strength of the sample, and F is the breaking load recorded at failure.

The mechanical properties and elastic modulus of the recycled carbon fiber composites were evaluated using a universal testing machine (ForceTek, Shanghai Scientific Instrument Co., Ltd, China). Specimen preparation was carried out in accordance with GB/T 3354-2014 and GB/T 30969-2014 standards. For each type of sample, at least five specimens were tested, and the corresponding force-strain curves were recorded. The tensile strength and shear strength of the resin-based composites were calculated using the following equations.

$$F^{\text{tu}} = \frac{P^{\text{max}}}{A} \quad (5)$$

$$\sigma_i = \frac{P_i}{A} \quad (6)$$

where F^{tu} represents the tensile strength (MPa), P^{max} is the maximum tensile load, σ_i denotes the tensile stress at the i -th data point (MPa), P_i is the corresponding force at the i -th data point (N), and A refers to the actual cross-sectional area of the specimen measured prior to testing (mm^2).

$$F^{\text{sbs}} = 0.75 \frac{P_m}{bh} \quad (7)$$

where F^{sbs} is the short-beam strength (MPa), P_m is the maximum applied load (N), b is the width at the midspan of the specimen measured prior to testing (mm), and h is the thickness at the midspan measured prior to testing (mm).

Results and discussion

Formulation and process selection

A clear quantitative relationship between degradation efficiency and reaction parameters was observed in the $\text{C}_8\text{H}_{10}\text{O}$ /TBD catalytic system. At a constant reaction time of 2 h, the degradation rate (DR) increased significantly with temperature ($150\text{--}200\text{ }^{\circ}\text{C}$). Complete degradation (DR = 100%) was achieved at $190\text{ }^{\circ}\text{C}$ with a mass ratio of $\text{C}_8\text{H}_{10}\text{O}:\text{TBD} = 30:1$, and this efficiency was maintained at $200\text{ }^{\circ}\text{C}$. In contrast, the same ratio resulted in only 68.56% degradation at $150\text{ }^{\circ}\text{C}$, confirming temperature as a critical factor.

Catalyst ratio also had a pronounced effect on degradation. At $190\text{ }^{\circ}\text{C}$, the 30:1 ratio resulted in complete degradation, while 20:1 and 50:1 ratios resulted in DRs of 87.18% and 74.87%, respectively. The 30:1 ratio exhibited optimal catalytic performance at $180\text{ }^{\circ}\text{C}$ (DR = 86.77%), demonstrating a distinct structure-activity relationship. Temperature-gradient

experiments further revealed that the impact of catalyst ratio became more pronounced at higher temperatures, with a 33% variation in the DR at 150 °C and an expanded range of 25–40% above 180 °C.

Overall, complete degradation with high energy efficiency was achieved at 190 °C and a mass ratio of $C_8H_{10}O$:TBD = 30 : 1 (TBD was used at a concentration of 0.25 mol L⁻¹). For resource-constrained scenarios, operation at 180 °C under the same ratio offers a more energy-efficient alternative, albeit with a longer reaction time.

Table 2 compares the catalytic performance of the system in this study with previously reported systems for resin degradation. Most reported strategies utilize alkaline or Lewis acid catalysts in polar solvents such as ethanol or ethylene glycol, typically under elevated temperatures (180–220 °C) and prolonged reaction times (4–10 h), achieving degradation ratios (DRs) ranging from 19.8% to 100%. Notably, KOH and ZnCl₂ afford DRs above 89% under relatively harsh conditions (200–220 °C, 4–5 h). The introduction of TBD (1,5,7-triazabicyclo[4.4.0]dec-5-ene) as an organic superbase significantly enhances the degradation efficiency, enabling complete degradation (100% DR) within 5 h at 180 °C using 4 wt% TBD in ethylene glycol.

In this study, β -phenylethanol is introduced for the first time as a solvent for resin degradation. When combined with 3 wt% TBD, the system achieves 86.8% DR at 180 °C in just 2 h and complete degradation at 190 °C within 2 h. This represents a substantial improvement in reaction efficiency and time over conventional systems. Furthermore, in previously reported systems using inorganic alkaline catalysts with organic solvents, DMSO is often required to improve catalyst solubility. However, the high toxicity and environmental persistence of DMSO pose additional concerns. In contrast, the system developed in this study eliminates the need for toxic co-solvents and can be reused multiple times until β -phenylethanol is exhausted.

Moreover, TBD and the resin degradation products can be effectively recovered *via* rotary evaporation. These features further enhance the sustainability of the process and are in better alignment with the principles of green chemistry.^{29,30}

To further clarify the advantages of the proposed recovery system, comparative experiments were conducted using the formulations of Experiments 5 and 6 from Table 2, under identical catalyst concentrations and a constant reaction time at 190 °C. The amounts of materials, experimental conditions,

Table 3 Experimental conditions and results for the control experiments

No.	C ₂ H ₆ O ₂ :TBD (wt:wt)	Temperature/°C	Time/h	DR/%
(K)	32:1	190	5	95.6
No.	C ₂ H ₆ O ₂ :NaOH (wt:wt)	Temperature/°C	Time/h	DR/%
(L)	111.3:1	190	5	26.76

and degradation rate results are summarized in Table 3, while other results are discussed in detail in the following sections.

For clarity and ease of reference, the experimental conditions are denoted using abbreviated labels, as summarized in Table 4.

Characterization of recycled carbon fibers

Surface morphology analysis by SEM. Before scanning electron microscopy (SEM) analysis, the virgin carbon fibers were washed with ethanol to ensure complete removal of sizing agents. As shown in Fig. 5(a–g), V-CF (Fig. 5a) exhibited a smooth surface with no visible resin residue. In contrast, 150-RCF (Fig. 5b) and 180-RCF (Fig. 5c) showed substantial particulate residues, indicating that the matrix resin was not completely removed under lower temperature conditions. With increasing treatment temperature, the fiber surfaces of 190-RCF (Fig. 5d) and 200-RCF (Fig. 5e) became significantly cleaner, and their morphology approached that of V-CF. However, the surface of 200-RCF exhibited pronounced grooves. In comparison, 190-RCF-T (Fig. 5f) still showed slight resin residue, while 190-RCF-N (Fig. 5g) displayed clear surface grooves and damage, possibly due to prolonged dissolution and chemical erosion. These results indicate that the treatment temperature, duration, and solvent/catalyst combination play critical roles in determining the surface integrity and cleanliness of the recovered carbon fibers.

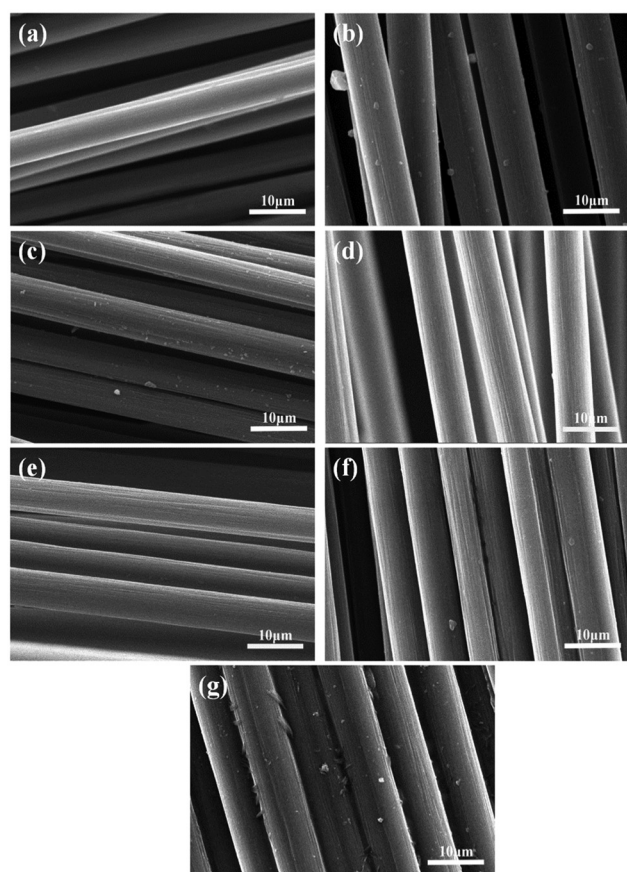
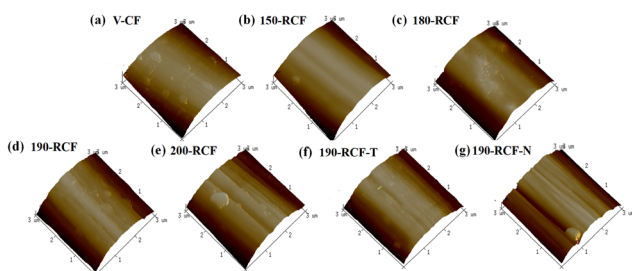
Surface morphology analysis by AFM. Surface structure analysis was conducted on the original carbon fibers and recycled carbon fibers subjected to different treatment conditions (Fig. 6). The surface of V-CF was relatively smooth with minimal defects, and the surface roughness (R_a) was only 80.7 nm. In contrast, recycled carbon fibers (RCFs) gradually exhibited longitudinal grooves aligned parallel to the fiber axis. With increasing degradation temperature and time, these grooves became more pronounced—both deeper and wider—

Table 2 Comparison of this work with other reported systems

No.	Catalyst (wt%)	Solvent	Temperature/time	DR/%	Ref.
1	KOH (30%)	Ethanol	200 °C, 4 h	89.3	29
2	Nitric acid (65%)	H ₂ O	80 °C, 10 h	100	29
3	ZnCl ₂ (20%)	Ethanol	220 °C, 5 h	89.9	29
4	MgCl ₂ (30%)	Ethanol	220 °C, 5 h	52.1	29
5	NaOH (1.25%)	Ethylene glycol	180 °C, 5 h	19.8	30
6	TBD (4%)	Ethylene glycol	180 °C, 5 h	93.6	30
7	TBD (3%)	β -Phenethyl alcohol	180 °C, 2 h	86.8	This work
8	TBD (3%)	β -Phenethyl alcohol	190 °C, 2 h	100	This work

Table 4 Summary of the experimental conditions and abbreviated labels

Code	Explanation
V-CF	Virgin carbon fiber
150-RCF	Recovered carbon fiber obtained at 150 °C with 0.25 mol L ⁻¹ TBD in β -phenylethanol for 2 h
180-RCF	Recovered carbon fiber obtained at 180 °C with 0.25 mol L ⁻¹ TBD in β -phenylethanol for 2 h
190-RCF	Recovered carbon fiber obtained at 190 °C with 0.25 mol L ⁻¹ TBD in β -phenylethanol for 2 h
200-RCF	Recovered carbon fiber obtained at 200 °C with 0.25 mol L ⁻¹ TBD in β -phenylethanol for 2 h
190-RCF-T	Recovered carbon fiber obtained at 190 °C with 0.25 mol L ⁻¹ TBD in ethylene glycol for 5 h
190-RCF-N	Recovered carbon fiber obtained at 190 °C with 0.25 mol L ⁻¹ NaOH in ethylene glycol for 5 h

**Fig. 5** Scanning electron micrographs of carbon fibers: (a) V-CF, (b) 150-RCF, (c) 180-RCF, (d) 190-RCF, (e) 200-RCF, (f) 190-RCF-T, and (g) 190-RCF-N.**Fig. 6** Topographical AFM images of carbon fibers: (a) V-CF, (b) 150-RCF, (c) 180-RCF, (d) 190-RCF, (e) 200-RCF, (f) 190-RCF-T, and (g) 190-RCF-N.

resulting in a significant increase in surface roughness. Although the roughened surface of RCFs may compromise the mechanical performance of the individual fibers, it can simultaneously enhance the interfacial adhesion between carbon fibers and the epoxy matrix, owing to improved mechanical interlocking and wettability.^{31,32} Notably, for the 190-RCF-N sample, in addition to the thermal degradation factors, the etching effect of NaOH on the fiber surface further intensified the roughness, elevating R_a to 139 nm, which may also contribute to potential performance trade-offs (Table 5).

Thermogravimetric analysis of recycled carbon fibers

The thermal stability of virgin carbon fibers (V-CFs) and regenerated carbon fibers (RCFs) recovered through different processes was evaluated by thermogravimetric analysis (TGA). As shown in Fig. 7, all samples exhibited a single-stage thermal decomposition behavior, which is primarily attributed to the degradation of surface residues or functional groups introduced during the recycling process. The V-CF displayed the highest thermal stability, retaining approximately 97.83% of its initial mass at 700 °C. In contrast, the residual mass of the RCFs decreased progressively with increasing recovery temperature, indicating that the carbon framework was subject to varying degrees of degradation or incorporation of thermally labile groups.

Specifically, the residual mass decreased from 96.63% (150-RCF) to 91.57% (200-RCF), highlighting the detrimental effect of elevated temperature on the structural stability of the carbon fibers. Notably, samples 190-RCF-T and 190-RCF-N showed further reductions in residual mass to 85.75% and 83.56%, respectively, suggesting that prolonged treatment time further compromised the structural integrity of the regenerated fibers. These findings demonstrate that although increasing the processing temperature facilitates the removal of the resin

Table 5 Summary of the R_a values of the carbon fibers before and after degradation

Samples	Surface roughness (nm)
V-CF	80.70
150-RCF	107.21
180-RCF	128.92
190-RCF	130.02
200-RCF	135.24
190-RCF-T	134.52
190-RCF-N	139.71

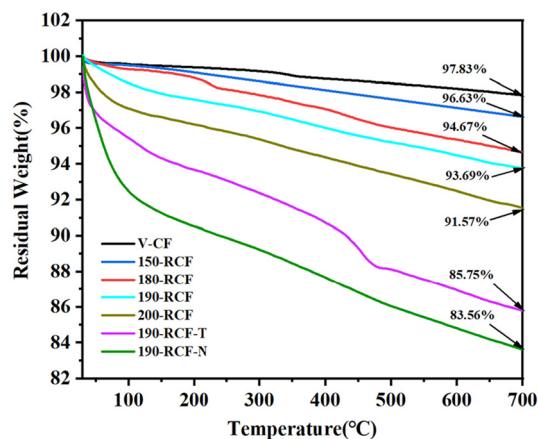


Fig. 7 TGA of virgin carbon fibres and recycled carbon fibres.

matrix, excessively high temperatures or extended reaction times may lead to the disruption of the carbon skeleton or oxidation of surface functional groups, ultimately reducing the thermal stability and mechanical performance of the regenerated carbon fibers. The underlying mechanisms will be further discussed based on subsequent characterization results.

Mechanical properties from single-fiber tensile testing

As shown in Fig. 8, compared with virgin carbon fiber (V-CF, 3254.99 MPa), the recovered carbon fibers treated at 150 °C and 180 °C retained approximately 96.6% and 95.3% of their original tensile strength, respectively. Even after treatment at 190 °C, a high strength retention of 94.9% was observed, while further increasing the temperature to 200 °C still resulted in a tensile strength retention of 92.9% (3025.76 MPa). These results indicate that thermal treatment below 200 °C effectively removes the matrix resin while largely preserving the mechanical integrity of the carbon fibers. In contrast, the tensile strength of sample 190-RCF-T decreased to 2827.33 MPa, corresponding to a retention of 86.9%, and that of 190-RCF-N

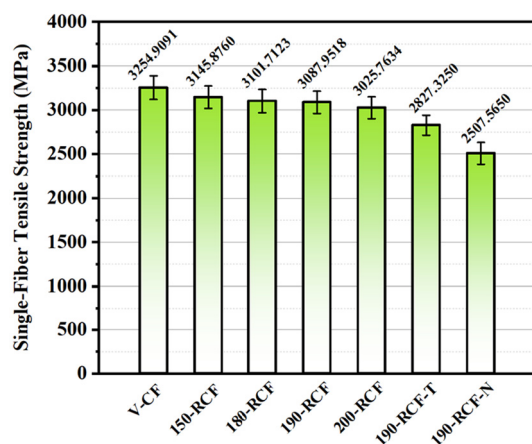


Fig. 8 Tensile strength of monofilaments of virgin and recycled carbon fibers.

dropped most significantly, with only 77.0% of the original strength maintained (2507.56 MPa). This trend is consistent with the SEM observations. Nevertheless, the reduction in tensile strength of the recovered carbon fibers remains non-negligible. In addition to surface degradation, internal crystallographic damage of the carbon fibers may also contribute to the mechanical deterioration. Therefore, the following sections will further investigate the evolution of the crystallographic structure and surface functional groups to elucidate the degradation mechanisms.

X-ray diffraction analysis

As illustrated in Fig. 9, all samples exhibit a distinct (002) diffraction peak, indicating that the recycled carbon fibers (RCFs) retain a well-defined graphitic structure. The interlayer spacing (d_{002}) of 190-RCF is 0.3473 nm, which is very close to that of virgin carbon fibers (V-CFs, 0.3466 nm), suggesting minimal disruption of the graphitic layers during the recycling process. In addition, 190-RCF shows a crystallite size (D) of 1.4350 nm and a D/d_{002} ratio of 4.1319, comparable to that of V-CF (3.9423), indicating that the crystalline order is well preserved under the optimized recycling conditions.

It is worth noting that the 200-RCF sample presents the smallest interlayer spacing (0.3448 nm), likely due to lattice contraction at elevated temperatures. Nevertheless, its D/d_{002} ratio (4.1099) remains close to that of 190-RCF, implying that the crystallite aspect ratio is not significantly affected. In contrast, the 180-RCF sample exhibits the largest crystallite size (1.5567 nm) and the highest D/d_{002} ratio (4.4679), reflecting an enhancement in structural ordering, despite a slightly increased interlayer spacing (0.3484 nm).

In addition, the 190-RCF-T sample demonstrates a well-maintained degree of graphitization and structural integrity. By contrast, the 190-RCF-N sample shows a relatively larger interlayer spacing (0.3495 nm) and the lowest D/d_{002} ratio (3.6861), suggesting a slight decline in graphitic ordering, which may be attributed to the introduction of sodium hydroxide or suboptimal reaction conditions.

Taken together, these results indicate that optimized recycling conditions effectively preserve the dimensional stability

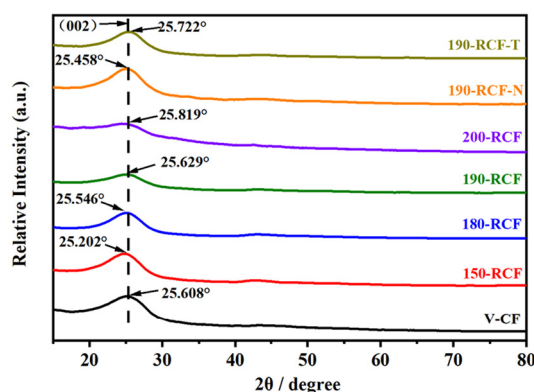


Fig. 9 XRD patterns of virgin and recycled carbon fibers.

and high degree of graphitization of carbon fibers. In combination with SEM observations and single-fiber tensile testing, the 190-RCF sample exhibits the most favorable overall performance among all recycled variants (Table 6).

X-ray photoelectron spectroscopy analysis

Fig. 10a presents the X-ray photoelectron spectroscopy (XPS) full spectrum, where three characteristic peaks are clearly observed, corresponding to C 1s (284.6 eV), O 1s (532.5 eV), and N 1s (400.5 eV). Table 7 summarizes the surface elemental composition of the original carbon fiber and the regenerated carbon fibers recovered under different conditions.

Deconvolution of the C 1s spectra revealed the presence of oxygen-containing functional groups. The peak at 284.6 eV was attributed to the C–C/C–H bonds, while peaks at 286.1 eV and 287.6 eV were assigned to the hydroxyl (C–O) and carbonyl (C=O) groups, respectively (Fig. 10b–h). The 180-RCF sample showed C–C and C–O contents similar to those of V-CF, with a slight decrease in the C=O content to 3.52%, indicating

Table 6 Crystallographic parameters of virgin and recycled carbon fibers

Samples	Parameters			
	2θ	d_{002} (nm)	D (nm)	D/d_{002}
V-CF	25.680	0.3466	1.3663	3.9423
150-RCF	25.202	0.3531	1.3547	3.8366
180-RCF	25.546	0.3484	1.5567	4.4679
190-RCF	25.629	0.3473	1.4350	4.1319
200-RCF	25.819	0.3448	1.4171	4.1099
190-RCF-N	25.722	0.3495	1.2886	3.6861
190-RCF-T	25.458	0.3460	1.3760	3.9764

Table 7 Surface elemental composition and relative content of oxygen-containing functional groups on virgin and recycled carbon fibers

Samples	Surface elemental composition (%)			Oxygenated groups (%)		
	C	N	O	C–C	C–O	C=O
V-CF	82.13	0.96	16.91	60.06	36.23	3.71
150-RCF	81.53	1.42	17.05	68.45	27.10	4.44
180-RCF	81.04	0.28	18.68	59.78	36.70	3.52
190-RCF	80.65	0.26	19.09	70.22	26.84	2.94
200-RCF	79.67	0.87	19.46	66.20	28.16	5.64
190-RCF-T	76.20	0.30	23.50	49.40	42.35	8.25
190-RCF-N	71.34	1.80	26.86	38.97	42.36	18.66

limited surface oxidation. When the regeneration temperature was increased to 190 °C (190-RCF), the C=O content further decreased to 2.94%, while the total oxygen content increased to 19.09%, suggesting that surface oxidation intensified with concurrent degradation of some carbonyl groups. Upon further heating to 200 °C (200-RCF), the C=O and O contents increased to 5.64% and 19.46%, respectively, likely due to surface reoxidation under high-temperature treatment. Notably, under the same 190 °C treatment, the surface oxidation of the 190-RCF-T sample was significantly enhanced, showing higher C–O (42.35%) and C=O (8.25%) contents, with the oxygen content rising to 23.50%. In contrast, the 190-RCF-N sample showed a dramatic increase in the C=O content to 18.66%, the oxygen content increased to 26.86%, while the C–C content significantly decreased to 38.97%.

These results clearly demonstrate the occurrence of surface oxidation during the recovery process, with the oxidation degree increasing with higher temperatures. This temperature-induced surface modification may introduce structural defects, leading to partial reduction in the tensile strength of the regenerated carbon fibers. Furthermore, different catalysts and treatment times play a key role in regulating the surface oxidation degree and the types of functional groups on carbon fibers.^{31,32}

Based on the above test results, β -phenethyl alcohol demonstrates superior degradation selectivity and milder reaction conditions compared to traditional ethylene glycol-based alcoholysis systems. β -Phenethyl alcohol not only efficiently cleaves the ester bonds in the anhydride-cured epoxy resin network but also significantly reduces damage to the carbon fiber surface. In contrast, ethylene glycol often leads to surface roughening, microcrack formation, and deterioration of mechanical properties. Although β -phenethyl alcohol is slightly more expensive, it offers a higher boiling point, lower vapor pressure, and lower corrosivity, resulting in safer operation, easier post-treatment, and stronger resin dissolution capability. By comparison, ethylene glycol, despite its low cost, requires a longer degradation time, causes more severe fiber damage, generates more toxic byproducts, and involves more complex downstream separation processes.

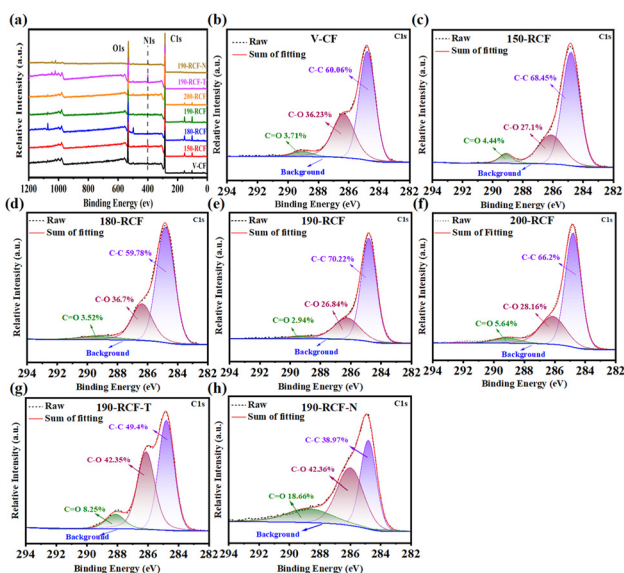


Fig. 10 XPS spectra of virgin and recycled carbon fibers: (a) survey spectra of all samples, (b) V-CF, (c) 150-RCF, (d) 180-RCF, (e) 190-RCF, (f) 200-RCF, (g) 190-RCF-T, and (h) 190-RCF-N.

FTIR and NMR characterization of the recovered solution and degradation products

Fig. 11b–e and 12 comprehensively illustrate the structural evolution of the anhydride-cured epoxy resin (DGEBA/MNA) during thermal degradation in a β -phenylethanol/TBD system at 190 °C over a period of 0–2 h. As shown in the FTIR spectra (Fig. 11b), the broad absorption band at 3200–3500 cm^{-1} , attributed to O–H stretching vibrations, gradually diminished over time, indicating nucleophilic substitution between hydroxyl groups and ester bonds in the resin matrix. Characteristic C–H stretching bands at 3027, 2943, and 2869 cm^{-1} correspond to aromatic, $-\text{CH}_2-$, and $-\text{CH}_3$ moieties, respectively. Aromatic skeletal vibrations at 1603 and 1496 cm^{-1} , along with fingerprint peaks at 854, 746, and 698 cm^{-1} , further confirm the presence of substituted phenyl rings. Notably, the peaks at 1045 and 1020 cm^{-1} , associated with C–O–C and C–O stretching, indicate that ether bonds underwent both cleavage and reformation, suggesting a dynamic depolymerization process.³³

Comparison with the FTIR spectrum of the cured resin (Fig. 11c) shows dominant ester carbonyl stretching at 1725–1740 cm^{-1} , aromatic C=C vibrations around 1600–1500 cm^{-1} , and ester/ether C–O stretching in the 1260–1020 cm^{-1} region. The absence of a distinct O–H peak near 3460 cm^{-1} suggests the formation of a highly crosslinked ester–aromatic network. After 2 h of degradation, a new O–H absorption band appeared, accompanied by enhanced aliphatic $-\text{CH}_3/-\text{CH}_2-$ signals and weakened aromatic and ether-related vibrations, indicating ester and ether bond cleavage and the formation of hydroxyl-containing low-molecular-weight compounds.³⁴

^{13}C NMR analysis (Fig. 11d) revealed resonance signals at $\delta = 140.0$, 128.6, and 126.3 ppm, corresponding to aromatic carbons, as well as signals at $\delta = 62.7$ ppm (β -phenylethanol $-\text{CH}_2-\text{OH}$) and 39.9 ppm (DGEBA tertiary carbon). The absence of carbon signals in the 150–180 ppm range suggests complete decarboxylation of the anhydride moieties under the catalytic action of TBD.³⁵ The ^1H NMR spectrum (Fig. 11e) displayed aromatic proton signals ($\delta = 7.0$ –7.3 ppm), $-\text{CH}_2-\text{OH}$ ($\delta = 3.6$ ppm), benzylic $-\text{CH}_2-$ ($\delta = 2.7$ ppm), and a broad O–H signal ($\delta = 4.7$ ppm), confirming the retention of the aromatic backbone and the formation of hydroxyl-terminated degradation fragments.^{36,37}

The GC–MS chromatogram (Fig. 12) further supports these findings. Seven major degradation products were identified: toluene, styrene, ethylbenzene, and benzaldehyde (peaks 1–4), resulting from backbone scission; benzyl alcohol (peak 5) and phthalic acid (peak 6), likely from β -phenylethanol oxidation and MNA ring-opening, respectively; and a bisphenol A-like compound (peak 7), indicating partial retention of the DGEBA framework. The abundant aromatic and hydroxyl-containing products observed are in strong agreement with the FTIR and NMR results, collectively confirming a degradation mechanism involving ester/ether bond cleavage, aromatic network breakdown, and incorporation of alcohol-derived functionalities under base-catalyzed conditions.

Based on FTIR, NMR, and GC–MS analyses, the degradation mechanism of anhydride-cured epoxy resin in the β -phenylethanol/TBD system and potential low-molecular-weight products were proposed (Table 8). The degradation pathway of the anhydride-cured epoxy resin in this system is illustrated in Fig. 13.

Reutilization potential of recycled carbon fibers

Based on the characterization results of the recycled carbon fibers, an optimized degradation process was developed using a β -phenylethanol/TBD mass ratio of 30 : 1 at 190 °C for 2 h. Under these conditions, the intrinsic structure of the fibers was well preserved. However, the recovered carbon fibers were all in the form of short, chopped fibers, which significantly limits their subsequent application potential.^{38,39}

To enhance the value-added utilization of recycled carbon fibers, a composite treatment strategy is proposed in this study. This approach integrates conventional sizing modification techniques with modern textile processing, enabling

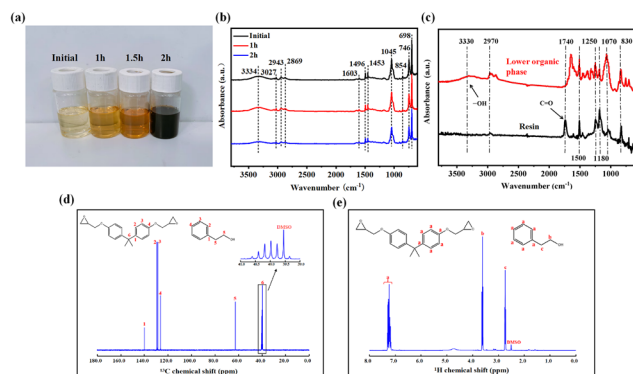


Fig. 11 FTIR and NMR characterization of the recovered solution and degradation products: (a) photographs of the recycling solutions at different degradation stages; (b) FTIR spectra of the recycling solutions at various degradation times; (c) comparison of the FTIR spectra between the cured DGEBA/MNA resin and its degradation products; (d) ^{13}C NMR spectrum of the recycling solution; and (e) ^1H NMR spectrum of the recycling solution.

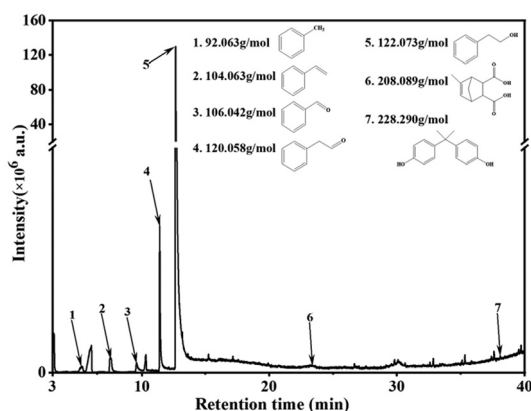
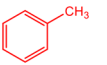
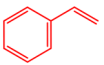
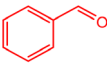
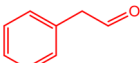
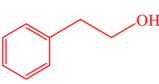
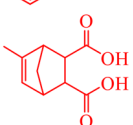
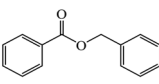
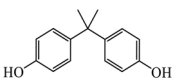
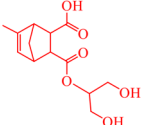
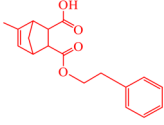
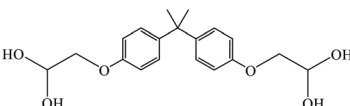
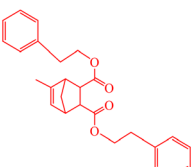
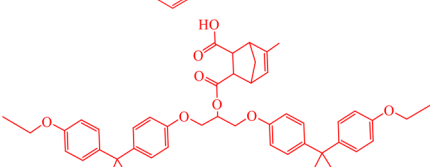
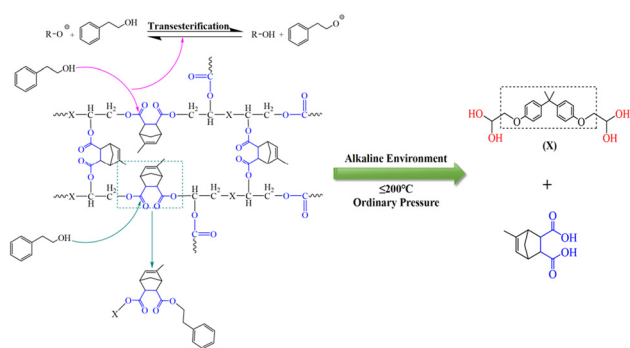


Fig. 12 GC–MS chromatogram of the degradation solution.

Table 8 Molecular structures of potential degradation products generated during the resin degradation process

No.	M (g mol ⁻¹)	Molecular structure	No.	M (g mol ⁻¹)	Molecular structure
(1)	92.06		(2)	104.06	
(3)	106.06		(4)	120.06	
(5)	122.06		(6)	209.19	
(7)	213.15		(8)	228.29	
(9)	282.27		(10)	312.34	
(11)	384.40				
(12)	417.50				
(13)	759.93				

**Fig. 13** Schematic diagram of the degradation mechanism.

the direct spinning of chopped fibers into yarns or the fabrication of continuous yarns through hybridization with other high-performance fibers. This strategy offers two major advantages: multiscale fiber hybridization effectively compensates for the mechanical limitations of short fibers and the controlled spinning process ensures excellent fiber alignment and

structural stability in the final products, as illustrated in Fig. 14(b).⁴⁰

The tensile and short-beam shear test results shown in Fig. 15(a–d) demonstrate that the composite laminates reinforced with recycled carbon fiber textile yarns retained 65.67% of the tensile strength and 57.76% of the shear strength of laminates made with virgin carbon fibers, whereas composites reinforced with randomly oriented recycled chopped fibers retained only 28.85% of the tensile strength and 31.35% of the shear strength. This significant disparity highlights the severe limitations imposed by insufficient fiber length and disordered dispersion on the mechanical performance of recycled carbon fibers. These findings further confirm the effectiveness of textile processing techniques and hybrid reinforcement strategies in overcoming these limitations.

The fracture surface morphologies shown in Fig. 15(e) and (f) further support these conclusions. The results indicate that recycled carbon fibers processed by textile technology not only maintained good orientation but also exhibited significantly enhanced interfacial bonding with the resin matrix. Additionally, this processing method effectively reduced the

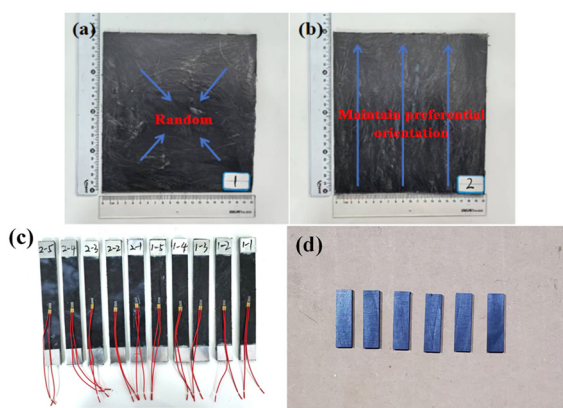


Fig. 14 Schematic illustrations of recycled carbon fiber-reinforced composite panels: (a) randomly oriented recycled short fiber composite panel, (b) textile-reinforced recycled carbon fiber composite panel, (c) tensile test samples, and (d) the short beam shear test specimen.

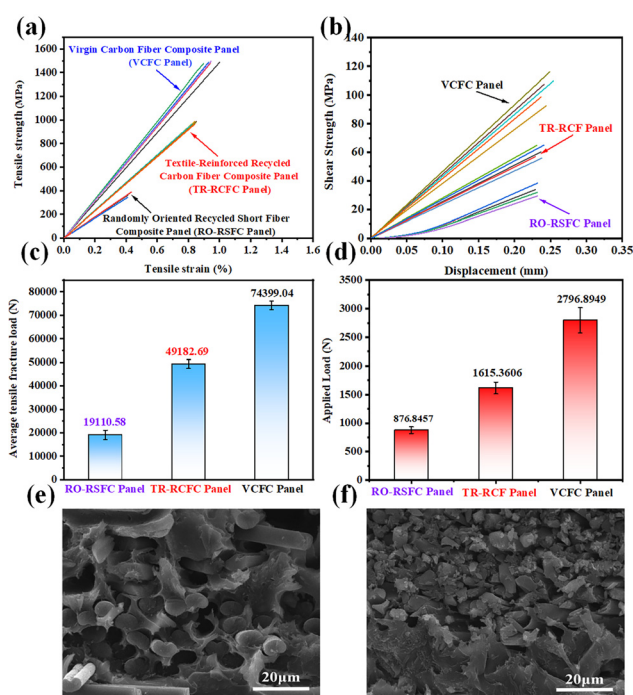


Fig. 15 Comparison of tensile test results: (a) tensile stress-strain curves, (b) shear stress-displacement curves, (c) average tensile failure load, (d) average shear failure load, (e) SEM image of the fracture surface of the laminate reinforced with randomly oriented recycled short fibers, and (f) SEM image of the fracture surface of the laminate reinforced with recycled carbon fiber textile yarns.

mechanical performance degradation caused by pore defects during composite preparation. These findings suggest that optimizing textile processing parameters and designing novel hybrid reinforcement systems could enable customized, high-value reuse of recycled carbon fiber products. This strategy not only improves the mechanical properties of the materials but also expands their application potential in structural engineering.^{18,41}

Conclusions

This study investigated the degradation behavior of anhydride-cured epoxy-based carbon fiber reinforced polymers (CFRPs) in β -phenethyl alcohol/TBD solutions. The experimental results demonstrated efficient CFRP decomposition under atmospheric pressure at 150–200 °C, with resin degradation rates rapidly increasing and stabilizing within 2 h. Although elevated temperatures intensified oxidation on the fiber surface, introducing some defects and partial structural weakening, the recycled fibers retained more than 93% of their original tensile strength, indicating excellent preservation of mechanical properties.

The alcohol solvent selectively cleaved the ester bonds in the resin's three-dimensional network, enabling efficient degradation of anhydride-cured epoxy composites, including thermoplastics, paints, sealants, and glass fibers. This method shows exceptional potential for the low-damage recovery of high-value materials, offering new possibilities for recycling contaminated CFRP waste. However, scaling this technology requires further research on TBD catalyst separation and reuse and solvent recycling, which are critical steps toward practical implementation in processing multi-contaminant CFRP waste and advancing sustainable composite recycling. The recovery of TBD may be achieved by synthesizing supported TBD catalysts, which can be reclaimed *via* filtration after resin degradation.⁴² This approach will be further explored in future studies.

Author contributions

Renlong Min and Chenyu Zhang contributed equally to this work. Renlong Min was responsible for the conceptualization, methodology development, experimental investigation, and preparation of the original draft. Chenyu Zhang contributed to formal analysis, data curation, and visualization. Haijuan Kong provided resources, acquired funding, and supervised the overall project. Shuo Liu performed validation and contributed to research supervision. Ziyao Peng was involved in project administration and participated in the review and editing of the manuscript. All authors have read and approved the final version of the manuscript.

Conflicts of interest

The authors declare that they have no known competing financial interests or personal relationships that could have appeared to influence the work reported in this paper.

Data availability

The data that support the findings of this study are available from the corresponding author upon reasonable request.

Acknowledgements

The authors sincerely acknowledge the material, technical, and financial support provided by Jiangsu Aosheng Composite Materials Technology. We also thank the Analytical and Testing Center of Shanghai University of Engineering Science for their assistance with testing and laboratory instrumentation. Constructive feedback and valuable discussions from colleagues during the course of this research are also deeply appreciated.

References

- 1 H. Ahmad, A. A. Markina, M. V. Porotnikov and F. Ahmad, A review of carbon fiber materials in automotive industry, *IOP Conf. Ser.: Mater. Sci. Eng.*, 2020, **971**(3), 032011.
- 2 S.-C. Lee, S.-T. Jeong, J.-N. Park, S.-J. Kim and G.-J. Cho, Study on Drilling Characteristics and Mechanical Properties of CFRP Composites, *Acta Mech. Solida Sin.*, 2008, **21**(4), 364–368.
- 3 A. Lefeuvre, S. Garnier, L. Jacquemin, B. Pillain and G. Sonnemann, Anticipating in-use stocks of carbon fiber reinforced polymers and related waste flows generated by the commercial aeronautical sector until 2050, *Resour., Conserv. Recycl.*, 2017, **125**, 264–272.
- 4 A. Lefeuvre, S. Garnier, L. Jacquemin, B. Pillain and G. Sonnemann, Anticipating in-use stocks of carbon fibre reinforced polymers and related waste generated by the wind power sector until 2050, *Resour., Conserv. Recycl.*, 2019, **141**, 30–39.
- 5 F. Meng, E. A. Olivetti, Y. Zhao, J. C. Chang, S. J. Pickering and J. McKechnie, Comparing Life Cycle Energy and Global Warming Potential of Carbon Fiber Composite Recycling Technologies and Waste Management Options, *ACS Sustainable Chem. Eng.*, 2018, **6**(8), 9854–9865.
- 6 A. M. Almushaikeh, S. O. Alaswad, M. S. Alsuhybani, B. M. Alotaibi, I. M. Alarifi, N. B. Alqahtani, S. M. Aldosari, S. S. Alsaleh, A. S. Haidyrah, A. A. Alolyan and B. A. Alshammari, Manufacturing of carbon fiber reinforced thermoplastics and its recovery of carbon fiber: A review, *Polym. Test.*, 2023, **122**, 108029.
- 7 M. Das and S. Varughese, A Novel Sonochemical Approach for Enhanced Recovery of Carbon Fiber from CFRP Waste Using Mild Acid–Peroxide Mixture, *ACS Sustainable Chem. Eng.*, 2016, **4**(4), 2080–2087.
- 8 C. E. Kouparitsas, C. N. Kartalis, P. C. Varelidis, C. J. Tsenoglou and C. D. Papaspyrides, Recycling of the fibrous fraction of reinforced thermoset composites, *Polym. Compos.*, 2004, **23**(4), 682–689.
- 9 M. A. Nahil and P. T. Williams, Recycling of carbon fibre reinforced polymeric waste for the production of activated carbon fibres, *J. Anal. Appl. Pyrolysis*, 2011, **91**(1), 67–75.
- 10 F. A. López, O. Rodríguez, F. J. Alguacil, I. García-Díaz, T. A. Centeno, J. L. García-Fierro and C. González, Recovery of carbon fibres by the thermolysis and gasification of waste prepreg, *J. Anal. Appl. Pyrolysis*, 2013, **104**, 675–683.
- 11 K. W. Kim, H. M. Lee, J. H. An, D. C. Chung, K. H. An and B. J. Kim, Recycling and characterization of carbon fibers from carbon fiber reinforced epoxy matrix composites by a novel super-heated-steam method, *J. Environ. Manag.*, 2017, **203**(Pt 3), 872–879.
- 12 G. Oliveux, L. O. Dandy and G. A. Leeke, Current status of recycling of fibre reinforced polymers: Review of technologies, reuse and resulting properties, *Prog. Mater. Sci.*, 2015, **72**, 61–99.
- 13 S. Karuppannan Gopalraj and T. Kärki, A review on the recycling of waste carbon fibre/glass fibre-reinforced composites: fibre recovery, properties and life-cycle analysis, *SN Appl. Sci.*, 2020, **2**(3), 433.
- 14 Y. Ren, L. Xu, X. Shang, Z. Shen, R. Fu, W. Li and L. Guo, Evaluation of Mechanical Properties and Pyrolysis Products of Carbon Fibers Recycled by Microwave Pyrolysis, *ACS Omega*, 2022, **7**(16), 13529–13537.
- 15 D. Borjan, Z. Knez and M. Knez, Recycling of Carbon Fiber-Reinforced Composites-Difficulties and Future Perspectives, *Materials*, 2021, **14**(15), 4191.
- 16 S. Pimenta and S. T. Pinho, Recycling carbon fibre reinforced polymers for structural applications: technology review and market outlook, *Waste Manag.*, 2011, **31**(2), 378–392.
- 17 J. Jiang, G. Deng, X. Chen, X. Gao, Q. Guo, C. Xu and L. Zhou, On the successful chemical recycling of carbon fiber/epoxy resin composites under the mild condition, *Compos. Sci. Technol.*, 2017, **151**, 243–251.
- 18 C. Shenghu, W. U. Zhis and W. Xin, Tensile Properties of CFRP and Hybrid FRP Composites at Elevated Temperatures, *J. Compos. Mater.*, 2009, **43**(4), 315–330.
- 19 O. Daglar, B. Alkan, U. S. Gunay, G. Hizal, U. Tunca and H. Durmaz, Ultrafast synthesis of phosphorus-containing polythioethers in the presence of TBD, *Eur. Polym. J.*, 2022, **162**, 110932.
- 20 J. Wu, Y. Pan, Z. Ruan, Z. Zhao, J. Ai, J. Ban and X. Jing, Carbon fiber-reinforced epoxy with 100% fiber recycling by transesterification reactions, *Front. Mater.*, 2022, **9**, 1045372.
- 21 B. Rijo, A. P. S. Dias and J. P. S. Carvalho, Recovery of carbon fibers from aviation epoxy composites by acid solvolysis, *Sustain. Mater. Technol.*, 2023, **35**, e00545.
- 22 C. Chaabani, E. Weiss-Hortala and Y. Soudais, Impact of Solvolysis Process on Both Depolymerization Kinetics of Nylon 6 and Recycling Carbon Fibers from Waste Composite, *Waste Biomass Valor.*, 2017, **8**(8), 2853–2865.
- 23 Z.-s. Tian, Y.-q. Wang and X.-l. Hou, Review of chemical recycling and reuse of carbon fiber reinforced epoxy resin composites, *New Carbon Mater.*, 2022, **37**(6), 1021–1041.
- 24 M. D. Hecker, M. L. Longana, O. Thomsen and I. Hamerton, Recycling of carbon fibre reinforced polymer composites with superheated steam – A review, *J. Cleaner Prod.*, 2023, **428**, 139320.
- 25 L. Liu, M. Du and F. Liu, Recent advances in interface microscopic characterization of carbon fiber-reinforced polymer composites, *Front. Mater.*, 2023, **10**, 1124338.

- 26 B. S. Maia, J. Tjong and M. Sain, Material characterization of recycled and virgin carbon fibers for transportation composites lightweighting, *Mater. Today Sustain.*, 2019, **5**, 100011.
- 27 P. Yang, Q. Zhou, X.-X. Yuan, J. M. N. van Kasteren and Y.-Z. Wang, Highly efficient solvolysis of epoxy resin using poly(ethylene glycol)/NaOH systems, *Polym. Degrad. Stab.*, 2012, **97**(7), 1101–1106.
- 28 W. Nie, J. Liu, W. Liu, J. Wang and T. Tang, Decomposition of waste carbon fiber reinforced epoxy resin composites in molten potassium hydroxide, *Polym. Degrad. Stab.*, 2015, **111**, 247–256.
- 29 T. Liu, M. Zhang, X. Guo, C. Liu, T. Liu, J. Xin and J. Zhang, Mild chemical recycling of aerospace fiber/epoxy composite wastes and utilization of the decomposed resin, *Polym. Degrad. Stab.*, 2017, **139**, 20–27.
- 30 X. Kuang, Q. Shi, Y. Zhou, Z. Zhao, T. Wang and H. J. Qi, Dissolution of epoxy thermosets via mild alcoholysis: the mechanism and kinetics study, *RSC Adv.*, 2018, **8**(3), 1493–1502.
- 31 W. Song, A. J. Gu, G. Z. Liang and L. Yuan, Effect of the surface roughness on interfacial properties of carbon fibers reinforced epoxy resin composites, *Appl. Surf. Sci.*, 2011, **257**(9), 4069–4074.
- 32 Y. C. Liang, X. H. Zhang, X. H. Wei, D. Q. Jing, W. G. Su and S. C. Zhang, Contribution of surface roughness and oxygen-containing groups to the interfacial shear strength of carbon fiber/epoxy resin composites, *New Carbon Mater.*, 2023, **38**(6), 118683.
- 33 M. Pannico, G. Mensitieri and P. Musto, *In situ* FTIR spectroscopy of epoxy resin degradation: kinetics and mechanisms, *Front. Chem.*, 2024, **12**, 1476965.
- 34 L. Ye, K. Wang, H. Feng and Y. Wang, Recycling of Carbon Fiber-reinforced Epoxy Resin-based Composites Using a Benzyl Alcohol/Alkaline System, *Fibers Polym.*, 2021, **22**(3), 811–818.
- 35 A. Venkatesh, M. P. Hanrahan and A. J. Rossini, Proton detection of MAS solid-state NMR spectra of half-integer quadrupolar nuclei, *Solid State Nucl. Magn. Reson.*, 2017, **84**, 171–181.
- 36 W. Y. Chen, Y. Z. Wang and F. C. Chang, Study on curing kinetics and curing mechanism of epoxy resin based on diglycidyl ether of bisphenol a and melamine phosphate, *J. Appl. Polym. Sci.*, 2004, **92**(2), 892–900.
- 37 Z.-y. Si, Z.-x. Sun, L.-w. Ye, A.-j. Gao and Y. Wang, Study on Degradation Mechanism of Carbon Fiber-reinforced Anhydride-cured Resin-based Matrix Composites by a Benzyl Alcohol/NaOH System, *Fibers Polym.*, 2022, **23**(11), 3188–3196.
- 38 K. Yanaze and N. Kihara, Preparation of Carbon Fiber-Reinforced Polymer Using Oxidatively Degradable Matrix Polymer: Recovery and Reuse of Carbon Fiber Sheet., *J. Appl. Polym. Sci.*, 2025, 56985.
- 39 L. Jeantet, A. Regazzi, D. Perrin, M. F. Pucci, S. Corn, J.-C. Quantin and P. Ienny, Recycled carbon fiber potential for reuse in carbon fiber/PA6 composite parts, *Composites, Part B*, 2024, **269**, 111100.
- 40 A. Salas, M. E. Berrio, S. Martel, A. Diaz-Gomez, D. A. Palacio, V. Tuninetti, C. Medina and M. F. Melendrez, Towards recycling of waste carbon fiber: Strength, morphology and structural features of recovered carbon fibers, *Waste Manag.*, 2023, **165**, 59–69.
- 41 P. Pomarède, L. Chehami, N. F. Declercq, F. Meraghni, J. Dong, A. Locquet and D. S. Citrin, Application of Ultrasonic Coda Wave Interferometry for Micro-cracks Monitoring in Woven Fabric Composites, *J. Nondestr. Eval.*, 2019, **38**(1), 26.
- 42 B. Karmakar, An Organobase (TBD)-Anchored Mesoporous Silica Nanoparticle-Catalyzed Green Synthesis of Dihydropyrano[2,3-*c*]pyrazoles, *Aust. J. Chem.*, 2016, **69**(10), CH15812.